Adaptive edge element approximation of H(curl)-elliptic optimal control problems with control constraints

Ronald H. W. Hoppe, Irwin Yousept

Adaptive edge element approximation of H(curl)-elliptic optimal control problems with control constraints

Ronald H. W. Hoppe · Irwin Yousept

Abstract A three-dimensional **H(curl)**-elliptic optimal control problem with distributed control and pointwise constraints on the control is considered. We present a residual-type a posteriori error analysis with respect to a curl-conforming edge element approximation of the optimal control problem. Here, the lowest order edge elements of Nédélec's first family are used for the discretization of the state and the control with respect to an adaptively generated family of simplicial triangulations of the computational domain. In particular, the a posteriori error estimator consists of element and face residuals associated with the state equation and the adjoint state equation. The main results are the reliability of the estimator and its efficiency up to oscillations in terms of the data of the problem. In the last part of the paper, numerical results are included which illustrate the performance of the adaptive approach.

R. H. W. Hoppe (✉)
Department of Mathematics, University of Houston, Houston, TX 77204-3008, USA
e-mail: rohop@math.uh.edu

R. H. W. Hoppe
Institute of Mathematics, University of Augsburg, 86159 Augsburg, Germany
e-mail: hoppe@math.uni-augsburg.de

I. Yousept
Graduate School of Excellence Computational Engineering, Technical University
Darmstadt, 64293 Darmstadt, Germany
e-mail: yousept@gsc.tu-darmstadt.de

1 Introduction

This paper is devoted to an a posteriori error analysis of adaptive edge element methods for control constrained distributed optimal control of $H(\mathbf{curl})$-elliptic problems in $\mathbb{R}^3$. Adaptive edge element methods for $H(\mathbf{curl})$-elliptic boundary value problems on the basis of residual-type a posteriori error estimators have been initiated in [6,7,28] and later on considered in [10,32]. A convergence analysis has been provided in [22]. For nonstandard discretizations such as Discontinuous Galerkin methods, we refer to [11,23]. In case of the time-harmonic Maxwell equations, convergence and quasi-optimality of adaptive edge element approximations have been established in [39,43] in the spirit of the results obtained in [12] for linear second order elliptic boundary value problems.

We refer to [1,4,5,15,31,37] for various approaches to adaptive finite element approximations and to [24,36,40–42] for recent results on the mathematical and numerical analysis of the optimal control of $H(\mathbf{curl})$-elliptic PDEs. To the best of our knowledge, this paper is the first contribution towards a residual-type a posteriori error analysis for $H(\mathbf{curl})$-elliptic optimal control problems. We are not aware of any previous studies in this direction. On the other hand, both residual-type a posteriori error estimators and dual weighted residuals for P1 conforming finite element approximations of control constrained $H^1(\Omega)$-elliptic optimal control problems have been developed in [16,18,25,26] and [17,38].

Adaptive finite element methods (AFEMs) typically consist of successive loops of the sequence

$$\text{SOLVE} \rightarrow \text{ESTIMATE} \rightarrow \text{MARK} \rightarrow \text{REFINE} . \tag{1.1}$$

The first step SOLVE stands for the efficient solution of the finite element discretized problem with respect to a given triangulation of the computational domain. Efficient iterative solvers include multilevel techniques and/or domain decomposition methods. As far as their application to edge element discretizations of $H(\mathbf{curl})$-elliptic problems is concerned, we refer to [2,19] (cf. also the survey articles [3,20] and the references therein). The second step ESTIMATE requires the a posteriori estimation of the global discretization error or some other error functional as a basis for an adaptive mesh refinement and will be in the focus of our paper. The following step MARK is devoted to the specification of elements of the triangulation that have to be selected for refinement in order to achieve a reduction of the error. Within the convergence analysis of AFEMs [8,12,14,33] a so-called bulk criterion, meanwhile also known as Dörfler marking, has been investigated which will be adopted here. Finally, the last step REFINE realizes the refinement of the mesh. Here, we will use the newest vertex bisection.

This paper is organized as follows: The optimal control problem will be stated in Sect. 2 with the optimality conditions being given in Sect. 2.1 in terms of the state, the adjoint state, the control, and the Lagrangian multiplier. The control problem is discretized with respect to a shape regular family of simplicial triangulations of the computational domain using curl-conforming edge elements of Nédélec's first family

for all relevant variables (see Sect. 2.2). The a posteriori error analysis involves a residual-type error estimator consisting of element and face residuals and oscillations associated with the data of the problem which will be introduced in Sect. 2.3. The marking of elements for refinement by Dörfler marking and the adaptive refinement by newest vertex bisection will be briefly described in Sect. 2.4. The main results, namely the reliability of the residual a posteriori error estimator and its efficiency up to data oscillations, will be established in Sects. 3 and 4. Finally, Sect. 5 contains a documentation of numerical results illustrating the performance of the adaptive approach.

2 The optimal control problem and its edge element approximation

2.1 The optimal control problem

We adopt standard notation from Lebesgue and Sobolev space theory (cf., e.g., [34]). In particular, for a bounded polyhedral domain $\Omega \subset \mathbb{R}^3$, we refer to $L^2(\Omega)$ and $H^m(\Omega)$, $m \in \mathbb{N}$, as the Hilbert space of Lebesgue integrable functions in Ω and the Sobolev space of functions with Lebesgue integrable generalized derivatives up to order m. Likewise, $\boldsymbol{L}^2(\Omega)$ and $\boldsymbol{H}^m(\Omega)$ stand for the corresponding Hilbert spaces of vector-valued functions. In both cases, the inner products and associated norms will be denoted by $(\cdot, \cdot)_{m,\Omega}$ and $\| \cdot \|_{m,\Omega}, m \geq 0$, respectively. For a function $v \in H^1(\Omega)$, we denote by $v|_\Gamma$, $\Gamma := \partial\Omega$, the trace of v on Γ and define $H_0^1(\Omega) := \{v \in H^1(\Omega) \mid v|_\Gamma = 0\}$. Moreover, we denote by $\boldsymbol{H}(\mathbf{curl}; \Omega) := \{\boldsymbol{v} \in \boldsymbol{L}^2(\Omega) \mid \mathbf{curl}\, \boldsymbol{v} \in \boldsymbol{L}^2(\Omega)\}$ and $\boldsymbol{H}(\mathrm{div}; \Omega) := \{\boldsymbol{v} \in \boldsymbol{L}^2(\Omega) \mid \mathrm{div}\, \boldsymbol{v} \in L^2(\Omega)\}$ the Hilbert spaces of vector-valued functions with the inner products $(\cdot, \cdot)_{\mathrm{curl},\Omega}, (\cdot, \cdot)_{\mathrm{div},\Omega}$ and associated norms $\| \cdot \|_{\mathrm{curl},\Omega}, \| \cdot \|_{\mathrm{div},\Omega}$. We refer to $\boldsymbol{H}_0(\mathbf{curl}; \Omega) := \{\boldsymbol{v} \in \boldsymbol{H}(\mathbf{curl}; \Omega) \mid \boldsymbol{\pi}_t(\boldsymbol{v}) = 0 \text{ on } \Gamma\}$ as the subspace of vector fields with vanishing tangential trace components $\boldsymbol{\pi}_t(\boldsymbol{v}) := \boldsymbol{n}_\Gamma \wedge (\boldsymbol{v} \wedge \boldsymbol{n}_\Gamma)$ on Γ, where $\boldsymbol{n}_\Gamma$ stands for the exterior unit normal vector on Γ. We further denote by $\boldsymbol{\gamma}_t(\boldsymbol{v}) := \boldsymbol{v} \wedge \boldsymbol{n}_\Gamma$ the tangential trace of $\boldsymbol{v}$ on Γ. We note that for $\boldsymbol{v} \in \boldsymbol{H}(\mathbf{curl}; \Omega)$ there holds $\boldsymbol{\pi}_t(\boldsymbol{v}) \in \boldsymbol{H}^{-1/2}(\mathbf{curl}_\Gamma; \Gamma)$ and $\boldsymbol{\gamma}_t(\boldsymbol{v}) \in \boldsymbol{H}^{-1/2}(\mathrm{div}_\Gamma; \Gamma)$, where $\mathbf{curl}_\Gamma$ and div_Γ stand for the tangential $\mathbf{curl}$ and the tangential div (cf., e.g., [9]).

We consider the following control constrained $\boldsymbol{H}(\mathbf{curl})$-elliptic optimal control problem: find $(\boldsymbol{y}, \boldsymbol{u}) \in \boldsymbol{V} \times \boldsymbol{K}$ such that

$$\min_{(\boldsymbol{y},\boldsymbol{u}) \in \boldsymbol{V} \times \boldsymbol{K}} J(\boldsymbol{y}, \boldsymbol{u}) := \frac{1}{2} \left\| \mathbf{curl}\, \boldsymbol{y} - \boldsymbol{y}^d \right\|_{0,\Omega}^2 + \frac{\alpha}{2} \left\| \boldsymbol{u} - \boldsymbol{u}^d \right\|_{0,\Omega}^2 \quad (2.1a)$$

subject to the state equation

$$\mathbf{curl}\mu^{-1}\mathbf{curl}\, \boldsymbol{y} + \sigma\boldsymbol{y} = \boldsymbol{f} + \boldsymbol{u} \quad \text{in } \Omega, \quad (2.1b)$$

$$\boldsymbol{\pi}_t(\boldsymbol{y}) = \boldsymbol{0} \quad \text{on } \Gamma. \quad (2.1c)$$

Here, $\Omega \subset \mathbb{R}^3$ stands for a bounded polyhedral domain with boundary $\Gamma = \partial\Omega$, $\boldsymbol{y}^d \in \boldsymbol{H}_0(\mathbf{curl}; \Omega)$, $\boldsymbol{u}^d \in \boldsymbol{L}^2(\Omega)$, $\alpha > 0$, and $\boldsymbol{f} \in \boldsymbol{L}^2(\Omega)$. Moreover, $\boldsymbol{V} := \boldsymbol{H}_0(\mathbf{curl}; \Omega)$, and $\boldsymbol{K} \subset \boldsymbol{L}^2(\Omega)$ denotes the closed, convex set

$$K := \left\{ u \in L^2(\Omega) \mid u(x) \geq \psi(x) \text{ a.e. in } \Omega \right\},$$

where $\psi \in L^2(\Omega)$ is a given vector field. To simplify the subsequent analysis, we assume $\psi \equiv 0$ which is not that much of a restriction, because the transformation $u \mapsto \hat{u} := u - \psi$ gives rise to a problem with $\hat{u} \geq 0$, but a modified right-hand side f and a modified shift control u^d. The functions $\mu, \sigma \in L^\infty(\Omega)$ are supposed to be piecewise polynomial satisfying $\mu(x) \geq \mu_0 > 0$ and $\sigma(x) \geq \sigma_0 > 0$ a.e. in Ω.

Under the above assumptions, it is easy to show that (2.1a)–(2.1c) admits a unique solution $(y^*, u^*) \in V \times K$. The necessary and sufficient optimality conditions invoke an adjoint state $p^* \in V$ and a multiplier $\lambda^* \in L^2(\Omega)$ such that the quadruple $(y^*, u^*, p^*, \lambda^*)$ satisfies the optimality system

$$a(y^*, q) = \ell_1(q), \quad \forall q \in V, \tag{2.2a}$$
$$a(p^*, q) = \ell_2(q), \quad \forall q \in V, \tag{2.2b}$$
$$u^* - u^d = \alpha^{-1}(p^* - \lambda^*), \tag{2.2c}$$
$$\lambda^* \in \partial I_K(u^*), \tag{2.2d}$$

where $\partial I_K : L^2(\Omega) \to 2^{L^2(\Omega)}$ denotes the subdifferential of the indicator function I_K of the constraint set K (cf., e.g., [21]). Moreover, $a : V \times V \to \mathbb{R}$ refers to the bilinear form

$$a(y, q) := \left(\mu^{-1}\mathbf{curl}\, y, \mathbf{curl}\, q \right)_{0,\Omega} + (\sigma y, q)_{0,\Omega}, \quad y, q \in V, \tag{2.3}$$

and the functionals $\ell_i \in V^*$, $i = 1, 2$, are given according to

$$\ell_1(q) := (f + u^*, q)_{0,\Omega}, \quad q \in V, \tag{2.4a}$$
$$\ell_2(q) := (y^d - \mathbf{curl}\, y^*, \mathbf{curl}\, q)_{0,\Omega}, \quad q \in V. \tag{2.4b}$$

We note that (2.2d) can be equivalently written as the variational inequality

$$(\lambda^*, v - u^*)_{0,\Omega} \leq 0, \quad v \in K,$$

and the complementarity problem

$$-\lambda^* \in L^2_+(\Omega), \quad u^* \in L^2_+(\Omega), \quad (\lambda^*, u^*)_{0,\Omega} = 0, \tag{2.5}$$

where $L^2_+(\Omega)$ refers to the nonnegative cone in $L^2(\Omega)$.

For the derivation of the optimality system (2.2a)–(2.2d) we refer to [35].

Remark 2.1 The state equation (2.1b)–(2.1c) is highly related to the eddy current model, in which case the magnetic induction is given by the rotation of the state, i.e., $\mathbf{B} = \mathbf{curl}\, y$. Therefore, from the application point of view, it is more important to optimize the rotation field $\mathbf{curl}\, y$ rather than the field y itself. This is the reason for choosing the tracking-type objective functional (2.1a) with respect to $\mathbf{curl}\, y$. In this

context, the field $\mathbf{y}^d$ could represent a desired magnetic induction or a target arising from some measurement.

2.2 Edge element approximation

We assume $(h_n)_{n\in\mathbb{N}_0}$ to be a strictly decreasing null sequence of positive real numbers and $(\mathcal{T}_h(\Omega))_{h_n}$ a nested family of simplicial triangulations of Ω such that μ and σ are elementwise polynomial on $\mathcal{T}_{h_0}(\Omega)$. For an element $T \in \mathcal{T}_h(\Omega)$, we denote by h_T the diameter of T and set $h := \max\{h_T \mid T \in \mathcal{T}_h(\Omega)\}$. For $D \subseteq \bar{\Omega}$, we refer to $\mathcal{N}_h(D)$, $\mathcal{E}_h(D)$, and $\mathcal{F}_h(D)$ as the sets of vertices, edges, and faces of $\mathcal{T}_h(\Omega)$ in D. For $F \in \mathcal{F}_h(D)$, we denote by h_F the diameter of F and by $\omega_F := \bigcup\{T \in \mathcal{T}_h(\Omega) \mid F \subset \partial T\}$ the patch consisting of the union of elements sharing F as a common face. In the sequel, for two mesh dependent quantities A and B we use the notation $A \lesssim B$, if there exists a constant $C > 0$ independent of h such that $A \leq CB$.

For the discrete approximation of (2.1a)–(2.1c), we use the edge elements of Nédélec's first family

$$Nd_1(T) := \left\{ \mathbf{q} : T \to \mathbb{R}^3 \mid \mathbf{q}(\mathbf{x}) = \mathbf{a} + \mathbf{b} \wedge \mathbf{x}, \ \forall \mathbf{x} \in T \right\},$$

which give rise to the curl-conforming edge element space [29,30]

$$Nd_{1,0}(\Omega; \mathcal{T}_h(\Omega)) := \left\{ \mathbf{q}_h \in \mathbf{H}_0(\mathbf{curl}; \Omega) \mid \mathbf{q}_h|_T \in Nd_1(T), \ \forall T \in \mathcal{T}_h(\Omega) \right\}. \quad (2.6)$$

Setting $\mathbf{V}_h := Nd_{1,0}(\Omega; \mathcal{T}_h(\Omega))$ and

$$\mathbf{K}_h := \{\mathbf{u}_h \in \mathbf{V}_h \mid \mathbf{u}_h \geq \mathbf{0} \text{ in } \Omega\},$$

the edge element approximation of the distributed optimal control problem (2.1a)–(2.1c) reads as follows: Find $(\mathbf{y}_h, \mathbf{u}_h) \in \mathbf{V}_h \times \mathbf{K}_h$ such that

$$\min_{(\mathbf{y}_h, \mathbf{u}_h)\in \mathbf{V}_h \times \mathbf{K}_h} J(\mathbf{y}_h, \mathbf{u}_h) := \frac{1}{2} \left\| \mathbf{curl}\, \mathbf{y}_h - \mathbf{y}^d \right\|_{0,\Omega}^2 + \frac{\alpha}{2} \left\| \mathbf{u}_h - \mathbf{u}_h^d \right\|_{0,\Omega}^2 \quad (2.7a)$$

$$\text{subject to} \quad a(\mathbf{y}_h, \mathbf{q}_h) = (\mathbf{u}_h, \mathbf{q}_h)_{0,\Omega}, \quad \forall \mathbf{q}_h \in \mathbf{V}_h, \quad (2.7b)$$

where $\mathbf{u}_h^d \in \mathbf{V}_h$ is some approximation of $\mathbf{u}^d$. The existence and uniqueness of a solution $(\mathbf{y}_h^*, \mathbf{u}_h^*) \in \mathbf{V}_h \times \mathbf{V}_h$ can be deduced as in the continuous regime. The discrete optimality system gives rise to a discrete adjoint state $\mathbf{p}_h^* \in \mathbf{V}_h$ and a discrete multiplier $\boldsymbol{\lambda}_h^* \in \mathbf{V}_h$ such that the quadruple $(\mathbf{y}_h^*, \mathbf{u}_h^*, \mathbf{p}_h^*, \boldsymbol{\lambda}_h^*)$ satisfies

$$a(\mathbf{y}_h^*, \mathbf{q}_h) = \ell_{1,h}(\mathbf{q}_h), \quad \forall \mathbf{q}_h \in \mathbf{V}_h, \quad (2.8a)$$

$$a(\mathbf{p}_h^*, \mathbf{q}_h) = \ell_{2,h}(\mathbf{q}_h), \quad \forall \mathbf{q}_h \in \mathbf{V}_h, \quad (2.8b)$$

$$\mathbf{u}_h^* - \mathbf{u}_h^d = \alpha^{-1}(\mathbf{p}_h^* - \boldsymbol{\lambda}_h^*), \quad (2.8c)$$

$$\boldsymbol{\lambda}_h^* \in \partial I_{\mathbf{K}_h}(\mathbf{u}_h^*). \quad (2.8d)$$

Here, the functionals $\ell_{i,h} : V_h \to \mathbb{R}$, $1 \le i \le 2$, are given by

$$\ell_{1,h}(\boldsymbol{q}_h) := (\boldsymbol{f} + \boldsymbol{u}_h^*, \boldsymbol{q}_h)_{0,\Omega}, \quad \boldsymbol{q}_h \in V_h, \tag{2.9a}$$

$$\ell_{2,h}(\boldsymbol{q}_h) := (\boldsymbol{y}^d - \mathbf{curl}\, \boldsymbol{y}_h^*, \mathbf{curl}\, \boldsymbol{q}_h)_{0,\Omega}, \quad \boldsymbol{q}_h \in V_h. \tag{2.9b}$$

We note that (2.8d) can be stated as the complementarity problem

$$\lambda_h^* \le 0\,, \; \boldsymbol{u}_h^* \ge 0\,, \; (\lambda_h^*, \boldsymbol{u}_h^*)_{0,\Omega} = 0. \tag{2.10}$$

Remark 2.2 Using (2.8c), the discrete multiplier λ_h^* can be formally eliminated such that (2.8d) reads

$$\boldsymbol{p}_h^* - \alpha(\boldsymbol{u}_h^* - \boldsymbol{u}_h^d) \in \partial I_{K_h}(\boldsymbol{u}_h^*). \tag{2.11}$$

In practice, the discrete optimality system (2.8a), (2.8b), (2.11) is solved by a projected gradient type method (cf. Sect. 5).

Remark 2.3 It is possible to use other discretizations for the control than edge element approximations as, for instance, a discretization by elementwise constants with respect to the triangulation $\mathcal{T}_h(\Omega)$, i.e., $\boldsymbol{u}_h \in \boldsymbol{W}_h := \{\boldsymbol{w}_h \in \boldsymbol{L}^2(\Omega)|\boldsymbol{w}_h|_T \in P_0(T)^3, T \in \mathcal{T}_h(\Omega)\}$. Then, $\boldsymbol{u}_h^d$ has to be chosen as an approximation of $\boldsymbol{u}^d$ in $\boldsymbol{W}_h$ and the discrete multiplier λ_h^* lives in $\boldsymbol{W}_h$ as well. However, the optimality condition (2.8c) takes the form $\boldsymbol{u}_h^* - \boldsymbol{u}_h^d = \alpha^{-1}(\boldsymbol{M}_h \boldsymbol{p}_h^* - \lambda_h^*)$ with an appropriately defined operator $\boldsymbol{M}_h : V_h \to \boldsymbol{W}_h$ which leads to an additional term in the a posteriori error estimator (cf. [18] for such an approach in case of residual a posteriori error estimators for the optimal control of control constrained second order elliptic boundary value problems).

2.3 The residual-type a posteriori error estimator

In our a posteriori error analysis, we assume that $\boldsymbol{f}$ satisfies

$$\boldsymbol{f}\,|_T \in \boldsymbol{H}(\mathrm{div}, T), \quad (\boldsymbol{n}_F \cdot \boldsymbol{f})|_F \in L^2(F), \quad F \in \mathcal{F}_h(T), \; T \in \mathcal{T}_h(\Omega). \tag{2.12}$$

The residual-type a posteriori error estimator η_h consists of element residuals and face residuals associated with the state Eq. (2.2a) and the adjoint Eq. (2.2b) according to

$$\eta_h := \left(\sum_{T \in \mathcal{T}_h(\Omega)} \eta_T^2 + \sum_{F \in \mathcal{F}_h(\Omega)} \eta_F^2 \right)^{1/2}, \quad \eta_T^2 := \sum_{i=1}^2 \left(\left(\eta_{y,T}^{(i)}\right)^2 + \left(\eta_{p,T}^{(i)}\right)^2 \right),$$

$$\eta_F^2 := \sum_{i=1}^2 \left(\left(\eta_{y,F}^{(i)}\right)^2 + \left(\eta_{p,F}^{(i)}\right)^2 \right). \tag{2.13}$$

Here, $\eta_{y,T}^{(i)}$ and $\eta_{p,T}^{(i)}$, $1 \le i \le 2$, are given by

$$\eta_{y,T}^{(1)} := h_T \left\| \boldsymbol{f} + \boldsymbol{u}_h^* - \mathbf{curl}\, \mu^{-1}\, \mathbf{curl}\, \boldsymbol{y}_h^* - \sigma \boldsymbol{y}_h^* \right\|_{0,T}, \qquad (2.14a)$$

$$\eta_{y,T}^{(2)} := h_T \left\| \mathrm{div}(\boldsymbol{f} - \sigma \boldsymbol{y}_h^*) \right\|_{0,T}, \qquad (2.14b)$$

$$\eta_{p,T}^{(1)} := h_T \left\| \mathbf{curl}\, \boldsymbol{y}^d - \mathbf{curl}\, \mu^{-1}\, \mathbf{curl}\, \boldsymbol{p}_h^* - \sigma \boldsymbol{p}_h^* \right\|_{0,T}, \qquad (2.14c)$$

$$\eta_{p,T}^{(2)} := h_T \left\| \mathrm{div}(\sigma \boldsymbol{p}_h^*) \right\|_{0,T}. \qquad (2.14d)$$

The face residuals $\eta_{y,F}^{(i)}$ and $\eta_{p,F}^{(i)}$, $1 \le i \le 2$, read as follows

$$\eta_{y,F}^{(1)} := h_F^{1/2} \left\| [\boldsymbol{\gamma}_t(\mu^{-1}\mathbf{curl}\, \boldsymbol{y}_h^*)]_F \right\|_{0,F}, \qquad (2.15a)$$

$$\eta_{y,F}^{(2)} := h_F^{1/2} \left\| \boldsymbol{n}_F \cdot [(\boldsymbol{f} + \boldsymbol{u}_h^* - \sigma \boldsymbol{y}_h^*)]_F \right\|_{0,F}, \qquad (2.15b)$$

$$\eta_{p,F}^{(1)} := h_F^{1/2} \left\| [\boldsymbol{\gamma}_t(\mu^{-1}\mathbf{curl}\, \boldsymbol{p}_h^* + \mathbf{curl}\, \boldsymbol{y}_h^*)]_F \right\|_{0,F}, \qquad (2.15c)$$

$$\eta_{p,F}^{(2)} := h_F^{1/2} \left\| \boldsymbol{n}_F \cdot [(\sigma \boldsymbol{p}_h^*)]_F \right\|_{0,F}, \qquad (2.15d)$$

where $[\boldsymbol{\gamma}_t(\mu^{-1}\mathbf{curl}\, \boldsymbol{q}_h)]_F$ and $[\boldsymbol{q}_h]_F$, $\boldsymbol{q}_h \in \boldsymbol{V}_h$, denote the jumps of $\boldsymbol{\gamma}_t(\mu^{-1}\mathbf{curl}\, \boldsymbol{q}_h)$ and $\boldsymbol{q}_h$ across $F = T_+ \cap T_-$, $T_\pm \in \mathcal{T}_h(\Omega)$.

We will show reliability of η_h up to data oscillations $osc_h(\boldsymbol{u}^d)$ and its efficiency up to data oscillations $osc_h(\boldsymbol{y}^d)$, $osc_h(\boldsymbol{u}^d)$, and $osc_h(\boldsymbol{f})$ as given by

$$osc_h\left(\boldsymbol{y}^d\right) := \left(\sum_{T \in \mathcal{T}_h(\Omega)} osc_T^2\left(\boldsymbol{y}^d\right) \right)^{1/2}, \qquad (2.16a)$$

$$osc_T\left(\boldsymbol{y}^d\right) := h_T \left\| \mathbf{curl}\left(\boldsymbol{y}^d - \boldsymbol{y}_h^d\right) \right\|_{0,T}, \quad T \in \mathcal{T}_h(\Omega),$$

$$osc_h\left(\boldsymbol{u}^d\right) := \left\| \boldsymbol{u}^d - \boldsymbol{u}_h^d \right\|_{0,\Omega}, \qquad (2.16b)$$

$$osc_h(\boldsymbol{f}) := \left(\sum_{T \in \mathcal{T}_h(\Omega)} osc_T^2(\boldsymbol{f}) \right)^{1/2}, \qquad (2.16c)$$

$$osc_T(\boldsymbol{f}) := h_T \|\boldsymbol{f} - \boldsymbol{f}_h\|_{\mathrm{div},T} + \sum_{F \in \mathcal{F}_h(T)} h_F \|\boldsymbol{n}_F \cdot [\boldsymbol{f} - \boldsymbol{f}_h]_F\|_{0,F}, \quad T \in \mathcal{T}_h(\Omega),$$

$$\qquad (2.16d)$$

where $\boldsymbol{y}_h^d$, $\boldsymbol{u}_h^d \in \boldsymbol{V}_h$ are approximations of $\boldsymbol{y}^d$ and $\boldsymbol{u}^d$. Furthermore, $\boldsymbol{f}_h$ is an elementwise polynomial approximation of $\boldsymbol{f}$.

2.4 Dörfler marking and refinement

In the step MARK of the adaptive cycle (1.1), elements of the simplicial triangulation $\mathcal{T}_h(\Omega)$ are marked for refinement according to the information provided by the a posteriori error estimator. With regard to convergence and quasi-optimality of AFEMs, the bulk criterion from [14], now also known as Dörfler marking, is a convenient choice. Here, we select a set $\mathcal{M}$ of elements such that for some $\theta \in (0, 1)$ there holds

$$\sum_{T \in \mathcal{M}} \left(\eta_T^2 + \frac{1}{2} \sum_{F \in \mathcal{F}_h(T)} \eta_F^2 \right) \geq \theta \sum_{T \in \mathcal{T}_h(\Omega)} \left(\eta_T^2 + \frac{1}{2} \sum_{F \in \mathcal{F}_h(T)} \eta_F^2 \right). \qquad (2.17)$$

Elements of the triangulation $\mathcal{T}_h(\Omega)$ that have been marked for refinement are subdivided by the newest vertex bisection.

3 Reliability of the error estimator

In this section, we prove reliability of the residual a posteriori error estimator η_h in the sense that it provides an upper bound for the global discretization error.

Theorem 3.1 *Let $(\boldsymbol{y}^*, \boldsymbol{u}^*, \boldsymbol{p}^*, \lambda^*)$ and $(\boldsymbol{y}_h^*, \boldsymbol{u}_h^*, \boldsymbol{p}_h^*, \lambda_h^*)$ be the unique solutions of (2.2a)–(2.2d) and (2.8a)–(2.8d), respectively. Further, let η_h and $osc_h(\boldsymbol{u}^d)$ be the residual error estimator and the data oscillation as given by (2.13) and (2.16b). Then, there holds*

$$\left\| \boldsymbol{y}^* - \boldsymbol{y}_h^* \right\|_{curl, \Omega} + \left\| \boldsymbol{p}^* - \boldsymbol{p}_h^* \right\|_{curl, \Omega} + \left\| \boldsymbol{u}^* - \boldsymbol{u}_h^* \right\|_{0, \Omega} + \left\| \lambda^* - \lambda_h^* \right\|_{0, \Omega} \lesssim \eta_h + osc_h(\boldsymbol{u}^d). \qquad (3.1)$$

The proof of (3.1) will be given by a series of lemmas. Here, our strategy to deal with the lack of Galerkin orthogonality is to introduce an intermediate state $\boldsymbol{y}(\boldsymbol{u}_h^*) \in V$ and an intermediate adjoint state $\boldsymbol{p}(\boldsymbol{u}_h^*) \in V$ as follows: Find $(\boldsymbol{y}(\boldsymbol{u}_h^*), \boldsymbol{p}(\boldsymbol{u}_h^*)) \in V \times V$ such that

$$a\left(\boldsymbol{y}(\boldsymbol{u}_h^*), \boldsymbol{q}\right) = \left(\boldsymbol{f} + \boldsymbol{u}_h^*, \boldsymbol{q}\right)_{0, \Omega}, \quad \forall \boldsymbol{q} \in V, \qquad (3.2a)$$

$$a\left(\boldsymbol{p}(\boldsymbol{u}_h^*), \boldsymbol{q}\right) = \left(\boldsymbol{y}^d - \mathbf{curl}\, \boldsymbol{y}(\boldsymbol{u}_h^*), \mathbf{curl}\, \boldsymbol{q}\right)_{0, \Omega}, \quad \forall \boldsymbol{q} \in V. \qquad (3.2b)$$

Choosing $\boldsymbol{q} = \boldsymbol{p}(\boldsymbol{u}_h^*) - \boldsymbol{p}^*$ in (3.2a) and $\boldsymbol{q} = \boldsymbol{y}(\boldsymbol{u}_h^*) - \boldsymbol{y}^*$ in (3.2b) and then using (2.2a)–(2.2b), it follows that

$$\left(\boldsymbol{p}^* - \boldsymbol{p}(\boldsymbol{u}_h^*), \boldsymbol{u}^* - \boldsymbol{u}_h^*\right)_{0, \Omega} = -\left\| \mathbf{curl}\left(\boldsymbol{y}^* - \boldsymbol{y}(\boldsymbol{u}_h^*)\right) \right\|_{0, \Omega}^2, \qquad (3.3)$$

and hence

$$\left(\boldsymbol{p}^* - \boldsymbol{p}(\boldsymbol{u}_h^*), \boldsymbol{u}^* - \boldsymbol{u}_h^*\right)_{0, \Omega} \leq 0. \qquad (3.4)$$

In order to establish the reliability of the a posteriori error estimator η_h, we split the discretization error $\boldsymbol{y}^* - \boldsymbol{y}_h^*$ and $\boldsymbol{p}^* - \boldsymbol{p}_h^*$ according to

$$\boldsymbol{y}^* - \boldsymbol{y}_h^* = \left(\boldsymbol{y}^* - \boldsymbol{y}(\boldsymbol{u}_h^*)\right) + \left(\boldsymbol{y}(\boldsymbol{u}_h^*) - \boldsymbol{y}_h^*\right),$$
$$\boldsymbol{p}^* - \boldsymbol{p}_h^* = \left(\boldsymbol{p}^* - \boldsymbol{p}(\boldsymbol{u}_h^*)\right) + \left(\boldsymbol{p}(\boldsymbol{u}_h^*) - \boldsymbol{p}_h^*\right),$$

and estimate the terms on the right-hand sides separately.

Lemma 3.1 *Let* $(\boldsymbol{y}^*, \boldsymbol{u}^*, \boldsymbol{p}^*, \lambda^*)$ *and* $(\boldsymbol{y}_h^*, \boldsymbol{u}_h^*, \boldsymbol{p}_h^*, \lambda_h^*)$ *be the unique solutions of* (2.2a)–(2.2d) *and* (2.8a)–(2.8d), *respectively. Further, let* $\boldsymbol{y}(\boldsymbol{u}_h^*) \in \boldsymbol{V}$ *and* $\boldsymbol{p}(\boldsymbol{u}_h^*) \in \boldsymbol{V}$ *be the intermediate state and intermediate adjoint state as given by* (3.2a)–(3.2b). *Then, there holds*

$$\left\| \boldsymbol{y}(\boldsymbol{u}_h^*) - \boldsymbol{y}^* \right\|_{curl,\Omega} \lesssim \left\| \boldsymbol{u}^* - \boldsymbol{u}_h^* \right\|_{0,\Omega}, \tag{3.5a}$$
$$\left\| \boldsymbol{p}(\boldsymbol{u}_h^*) - \boldsymbol{p}^* \right\|_{curl,\Omega} \lesssim \left\| \boldsymbol{y}^* - \boldsymbol{y}(\boldsymbol{u}_h^*) \right\|_{0,\Omega}. \tag{3.5b}$$

Proof The results are immediate consequences of the $\boldsymbol{V}$-ellipticity and boundedness of $a(\cdot, \cdot)$. □

Our goal now is to estimate the terms $\| \boldsymbol{y}(\boldsymbol{u}_h^*) - \boldsymbol{y}_h^* \|_{curl,\Omega}$ and $\| \boldsymbol{p}(\boldsymbol{u}_h^*) - \boldsymbol{p}_h^* \|_{curl,\Omega}$, where the main key tool for the estimate is the Schöberl quasi-interpolation operator $\boldsymbol{\Pi}_h : \boldsymbol{V} \to \boldsymbol{V}_h$. In view of [32, Theorem 1], for every $\boldsymbol{v} \in \boldsymbol{V}$, we can decompose $\boldsymbol{v} - \boldsymbol{\Pi}_h \boldsymbol{v}$ into

$$\boldsymbol{v} - \boldsymbol{\Pi}_h \boldsymbol{v} = \nabla \varphi + \boldsymbol{z}, \tag{3.6}$$

where $\varphi \in H_0^1(\Omega)$ and $\boldsymbol{z} \in \boldsymbol{V}$ satisfy

$$h_T^{-1} \|\varphi\|_{0,T} + \|\nabla \varphi\|_{0,T} \lesssim \|\boldsymbol{v}\|_{0,\omega_T}, \tag{3.7a}$$
$$h_T^{-1} \|\boldsymbol{z}\|_{0,T} + \|\textbf{curl } \boldsymbol{z}\|_{0,T} \lesssim \|\textbf{curl } \boldsymbol{v}\|_{0,\omega_T}. \tag{3.7b}$$

Here, the element patches $\omega_T, T \in \mathcal{T}_h(\Omega)$, are given by

$$\omega_T := \cup \left\{ T' \in \mathcal{T}_h \mid T' \cap \tilde{\omega}_T \neq \emptyset \right\}, \quad \tilde{\omega}_T := \cup \left\{ T' \in \mathcal{T}_h \mid \mathcal{N}_h(T') \cap \mathcal{N}_h(T) \neq \emptyset \right\}.$$

Lemma 3.2 *Let* $(\boldsymbol{y}_h^*, \boldsymbol{u}_h^*, \boldsymbol{p}_h^*, \lambda_h^*)$ *be the unique solution of* (2.8a)–(2.8d), *and let* $\boldsymbol{y}(\boldsymbol{u}_h^*) \in \boldsymbol{V}$ *and* $\boldsymbol{p}(\boldsymbol{u}_h^*) \in \boldsymbol{V}$ *be the intermediate state and intermediate adjoint state as given by* (3.2a)–(3.2b). *Then, there holds*

$$\left\| \boldsymbol{y}(\boldsymbol{u}_h^*) - \boldsymbol{y}_h^* \right\|_{curl,\Omega} + \left\| \boldsymbol{p}(\boldsymbol{u}_h^*) - \boldsymbol{p}_h^* \right\|_{curl,\Omega} \lesssim \eta_h. \tag{3.8}$$

Proof In view of (2.2a) and (3.2a), for $\tilde{\boldsymbol{e}}_y := \boldsymbol{y}(\boldsymbol{u}_h^*) - \boldsymbol{y}_h^*$, the Galerkin orthogonality

$$a(\tilde{\boldsymbol{e}}_y, \boldsymbol{q}_h) = 0, \quad \forall \boldsymbol{q}_h \in \boldsymbol{V}_h,$$

holds true, from which we deduce

$$\|\tilde{e}_y\|^2_{curl,\Omega} \lesssim a\left(\tilde{e}_y, \tilde{e}_y - \Pi_h\tilde{e}_y\right)$$
$$= a\left(y(u^*_h), \tilde{e}_y - \Pi_h\tilde{e}_y\right) - a\left(y^*_h, \tilde{e}_y - \Pi_h\tilde{e}_y\right)$$
$$= \left(f + u^*_h, \tilde{e}_y - \Pi_h\tilde{e}_y\right)_{0,\Omega} - a\left(y^*_h, \tilde{e}_y - \Pi_h\tilde{e}_y\right)$$
$$= \left(f + u^*_h - \sigma y^*_h, \tilde{e}_y - \Pi_h\tilde{e}_y\right)_{0,\Omega} - \left(\mu^{-1}\mathbf{curl}\,y^*_h, \mathbf{curl}(\tilde{e}_y - \Pi_h\tilde{e}_y)\right)_{0,\Omega}.$$
$$(3.9)$$

Using the decomposition (3.6) with $v = \tilde{e}_y$ in (3.9) along with (3.7a)–(3.7b), (2.12), and the finite overlap of the element patches $\omega_T, T \in \mathcal{T}_h(\Omega)$, results in

$$\left\|y(u^*_h) - y^*_h\right\|^2_{curl,\Omega} \lesssim \sum_{T\in\mathcal{T}_h(\Omega)} \eta^2_{y,T} + \sum_{F\in\mathcal{F}_h(\Omega)} \eta^2_{y,F}. \qquad (3.10)$$

On the other hand, in view of (2.8b) and (3.2b), for $\tilde{e}_p := p(u^*_h) - p^*_h$ we obtain

$$\|\tilde{e}_p\|^2_{curl,\Omega} \lesssim a(\tilde{e}_p, \tilde{e}_p) = a(\tilde{e}_p, \Pi_h\tilde{e}_p) + a(\tilde{e}_p, \tilde{e}_p - \Pi_h\tilde{e}_p)$$
$$= (\mathbf{curl}(y^*_h - y(u^*_h)), \mathbf{curl}\,\Pi_h\tilde{e}_p)_{0,\Omega} + (y^d - \mathbf{curl}\,y(u^*_h), \mathbf{curl}(\tilde{e}_p - \Pi_h\tilde{e}_p))_{0,\Omega}$$
$$- a(p^*_h, \tilde{e}_p - \Pi_h\tilde{e}_p)$$
$$= (\mathbf{curl}(y^*_h - y(u^*_h)), \mathbf{curl}(\Pi_h\tilde{e}_p - \tilde{e}_p))_{0,\Omega} + (\mathbf{curl}(y^*_h - y(u^*_h)), \mathbf{curl}\,\tilde{e}_p)_{0,\Omega}$$
$$+ (y^d - \mathbf{curl}\,y(u^*_h), \mathbf{curl}(\tilde{e}_p - \Pi_h\tilde{e}_p))_{0,\Omega} - a(p^*_h, \tilde{e}_p - \Pi_h\tilde{e}_p)$$
$$= (\mathbf{curl}(y^*_h - y(u^*_h)), \mathbf{curl}\,\tilde{e}_p)_{0,\Omega} + (y^d - \mathbf{curl}\,y^*_h, \mathbf{curl}(\tilde{e}_p - \Pi_h\tilde{e}_p))_{0,\Omega}$$
$$- a(p^*_h, \tilde{e}_p - \Pi_h\tilde{e}_p)$$
$$= (\mathbf{curl}(y^*_h - y(u^*_h)), \mathbf{curl}\,\tilde{e}_p)_{0,\Omega} + (y^d - \mu^{-1}\mathbf{curl}\,p^*_h - \mathbf{curl}\,y^*_h, \mathbf{curl}(\tilde{e}_p$$
$$- \Pi_h\tilde{e}_p))_{0,\Omega} - (\sigma p^*_h, \tilde{e}_p - \Pi_h\tilde{e}_p)_{0,\Omega}. \qquad (3.11)$$

Then, using again the decomposition (3.6) with $v = \tilde{e}_p$ in (3.11) along with (3.7a)–(3.7b) and the finite overlap of the element patches $\omega_T, T \in \mathcal{T}_h(\Omega)$, it follows that

$$\left\|p(u^*_h) - p^*_h\right\|^2_{curl,\Omega} \lesssim \left\|y(u^*_h) - y^*_h\right\|^2_{curl,\Omega} + \sum_{T\in\mathcal{T}_h(\Omega)} \eta^2_{p,T} + \sum_{F\in\mathcal{F}_h(\Omega)} \eta^2_{p,F}. \qquad (3.12)$$

Finally, combining (3.10) and (3.12) allows to conclude (3.8). □

Lemma 3.3 *Let $(y^*, u^*, p^*, \lambda^*)$ and $(y^*_h, u^*_h, p^*_h, \lambda^*_h)$ be the unique solutions of (2.2a)–(2.2d) and (2.8a)–(2.8d), respectively. Furthermore, let η_h as well as $osc_h(u^d)$ be the residual-type a posteriori error estimator and data oscillation as given by (2.13) and (2.16b). Then, there holds*

$$\left\|u^* - u^*_h\right\|_{0,\Omega} + \left\|\lambda^* - \lambda^*_h\right\|_{0,\Omega} \lesssim \eta_h + osc_h(u^d). \qquad (3.13)$$

Proof Taking (2.2c) and (2.8c) into account, we find

$$\alpha \left\| u^* - u_h^* \right\|_{0,\Omega}^2 = \left(\lambda_h^* - \lambda^*, u^* - u_h^* \right)_{0,\Omega}$$
$$+ \left(p^* - p_h^*, u^* - u_h^* \right)_{0,\Omega} + \alpha \left(u^d - u_h^d, u^* - u_h^* \right)_{0,\Omega}. \quad (3.14)$$

Using (2.5) and (2.10), for the first term on the right-hand side in (3.14) it follows that

$$\left(\lambda_h^* - \lambda^*, u^* - u_h^* \right)_{0,\Omega}$$
$$= \underbrace{\left(\lambda_h^*, u^* \right)_{0,\Omega}}_{\leq 0} - \underbrace{\left(\lambda_h^*, u_h^* \right)_{0,\Omega}}_{= 0} - \underbrace{\left(\lambda^*, u^* \right)_{0,\Omega}}_{= 0} + \underbrace{\left(\lambda^*, u_h^* \right)_{0,\Omega}}_{\leq 0} \leq 0. \quad (3.15)$$

For the second and third term on the right-hand side in (3.14), in view of (3.4) and (3.8), an application of Young's inequality yields

$$\left(p^* - p_h^*, u^* - u_h^* \right)_{0,\Omega} = \underbrace{\left(p^* - p(u_h^*), u^* - u_h^* \right)_{0,\Omega}}_{\leq 0} + \left(p(u_h^*) - p_h^*, u^* - u_h^* \right)_{0,\Omega}$$

$$\leq \frac{\alpha}{4} \left\| u^* - u_h^* \right\|_{0,\Omega}^2 + \frac{1}{\alpha} \left\| p(u_h^*) - p_h^* \right\|_{0,\Omega}^2 \lesssim \frac{\alpha}{4} \left\| u^* - u_h^* \right\|_{0,\Omega}^2 + \frac{1}{\alpha} \eta_h^2, \quad (3.16a)$$

$$\alpha \left(u^d - u_h^d, u^* - u_h^* \right)_{0,\Omega} \leq \frac{\alpha}{4} \left\| u^* - u_h^* \right\|_{0,\Omega}^2 + \alpha \left\| u^d - u_h^d \right\|_{0,\Omega}^2. \quad (3.16b)$$

Using (3.15) and (3.16a), (3.16b) in (3.14) gives

$$\left\| u^* - u_h^* \right\|_{0,\Omega}^2 \lesssim \frac{2}{\alpha^2} \eta_h^2 + 2 osc_h^2 \left(u^d \right). \quad (3.17)$$

On the other hand, observing (2.2c) and (2.8c) as well as (3.5a), (3.5b), (3.8), and (3.17), for $\lambda^* - \lambda_h^*$ we obtain

$$\left\| \lambda^* - \lambda_h^* \right\|_{0,\Omega}^2 \leq 3 \left\| p^* - p_h^* \right\|_{0,\Omega}^2 + 3\alpha^2 \left\| u^* - u_h^* \right\|_{0,\Omega}^2 + 3\alpha^2 \left\| u^d - u_h^d \right\|_{0,\Omega}^2$$

$$\leq 3 \left(\left\| u^* - u_h^* \right\|_{0,\Omega} + \left\| p(u_h^*) - p_h^* \right\|_{0,\Omega} \right)^2 + 3\alpha^2 \left\| u^* - u_h^* \right\|_{0,\Omega}^2 + 3\alpha^2 \left\| u^d - u_h^d \right\|_{0,\Omega}^2$$

$$\lesssim (6 + 3\alpha^2) \left\| u^* - u_h^* \right\|_{0,\Omega}^2 + 6\eta_h^2 + 3\alpha^2 osc_h^2 \left(u^d \right)$$

$$\lesssim \left(\frac{2(6 + 3\alpha^2)}{\alpha^2} + 6 \right) \eta_h^2 + 3(4 + 3\alpha^2) osc_h^2 \left(u^d \right). \quad (3.18)$$

The assertion now follows from (3.17) and (3.18). $\qquad \square$

4 Efficiency of the error estimator

We establish the efficiency of η_h by means of the local bubble functions

$$b_T := 256 \prod_{i=1}^{4} \lambda_i^T, \quad b_F := 27 \prod_{i=1}^{3} \lambda_{F_i}^T.$$

Here, λ_i^T, $1 \leq i \leq 4$, are the barycentric coordinates of $T \in \mathcal{T}_h(\Omega)$ associated with the vertices of T, and $\lambda_{F_i}^T$, $1 \leq i \leq 3$, are the barycentric coordinates associated with the vertices of $F \in \mathcal{F}_h(\Omega)$. The norm equivalences

$$\left\| b_T^{1/2} p_h \right\|_{0,T} \leq \| p_h \|_{0,T} \lesssim \left\| b_T^{1/2} p_h \right\|_{0,T}, \quad p_h \in P_k(T), \ k \in \mathbb{N}, \tag{4.1a}$$

$$\left\| b_F^{1/2} p_h \right\|_{0,F} \leq \| p_h \|_{0,F} \lesssim \left\| b_F^{1/2} p_h \right\|_{0,F}, \quad p_h \in P_k(F), \ k \in \mathbb{N}, \tag{4.1b}$$

can be easily verified by an affine invariance argument.

Theorem 4.1 *Let $(y^*, u^*, p^*, \lambda^*)$ and $(y_h^*, u_h^*, p_h^*, \lambda_h^*)$ be the unique solutions of (2.2a)–(2.2d) and (2.8a)–(2.8d), respectively. Furthermore, let η_h and $osc_h(y^d)$, $osc_h(f)$ be the residual-type a posteriori error estimator and data oscillations as given in (2.13), (2.16a), and (2.16c). Then, there holds*

$$\eta_h \lesssim \| y^* - y_h^* \|_{curl,\Omega} + \| p^* - p_h^* \|_{curl,\Omega} + \| u^* - u_h^* \|_{0,\Omega} + osc_h\left(y^d\right) + osc_h\left(f\right). \tag{4.2}$$

The proof of the theorem will be given by a series of lemmas where we show local efficiency in the sense that-up to data oscillations—the element and face residuals can be bounded from above by the elementwise or patchwise discretization error.

Lemma 4.1 *Under the assumptions of Theorem 4.1, there holds*

$$\eta_{y,T}^{(1)} \lesssim \| y^* - y_h^* \|_{curl,T} + h_T \| u^* - u_h^* \|_{0,T} + osc_T(f), \tag{4.3a}$$

$$\eta_{p,T}^{(1)} \lesssim \| y^* - y_h^* \|_{curl,T} + \| p^* - p_h^* \|_{curl,T} + osc_T\left(y^d\right), \tag{4.3b}$$

for every $T \in \mathcal{T}_h(\Omega)$.

Proof Obviously, for every $T \in \mathcal{T}_h(\Omega)$, we have

$$\left(\eta_{y,T}^{(1)}\right)^2 \leq 2 \left(h_T^2 \left\| f_h + u_h^* - \mathbf{curl}\, \mu^{-1}\, \mathbf{curl}\, y_h^* - \sigma y_h^* \right\|_{0,T}^2 + osc_T^2(f) \right). \tag{4.4}$$

The function $z_h := (f_h + u_h^* - \mathbf{curl}\, \mu^{-1}\, \mathbf{curl}\, y_h^* - \sigma y_h^*) b_T$ is an admissible test function in (2.2a), and hence, applying (4.1a) and Stokes' theorem results in

$$h_T^2 \| \boldsymbol{f}_h + \boldsymbol{u}_h^* - \mathbf{curl}\, \mu^{-1}\, \mathbf{curl}\, \boldsymbol{y}_h^* - \sigma \boldsymbol{y}_h^* \|_{0,T}^2$$

$$\lesssim h_T^2 \left(\boldsymbol{f}_h + \boldsymbol{u}_h^* - \mathbf{curl}\, \mu^{-1}\, \mathbf{curl}\, \boldsymbol{y}_h^* - \sigma \boldsymbol{y}_h^*, \boldsymbol{z}_h \right)_{0,T}$$

$$= h_T^2 \left((\boldsymbol{f} + \boldsymbol{u}^*, \boldsymbol{z}_h)_{0,T} - a(\boldsymbol{y}_h^*, \boldsymbol{z}_h) + (\boldsymbol{u}_h^* - \boldsymbol{u}^*, \boldsymbol{z}_h)_{0,T} + (\boldsymbol{f}_h - \boldsymbol{f}, \boldsymbol{z}_h)_{0,T} \right)$$

$$= h_T^2 \left(a(\boldsymbol{y}^* - \boldsymbol{y}_h^*, \boldsymbol{z}_h) + (\boldsymbol{u}_h^* - \boldsymbol{u}^*, \boldsymbol{z}_h)_{0,T} + (\boldsymbol{f}_h - \boldsymbol{f}, \boldsymbol{z}_h)_{0,T} \right)$$

$$\lesssim h_T^2 \left(\| \boldsymbol{y}^* - \boldsymbol{y}_h^* \|_{curl,T} \| \boldsymbol{z}_h \|_{curl,T} + \left(\| \boldsymbol{u}^* - \boldsymbol{u}_h^* \|_{0,T} + \| \boldsymbol{f}_h - \boldsymbol{f} \|_{0,T} \right) \| \boldsymbol{z}_h \|_{0,T} \right).$$

Finally, using Young's inequality, the inverse inequality

$$\| \boldsymbol{z}_h \|_{curl,T} \lesssim h_T^{-1} \| \boldsymbol{z}_h \|_{0,T}, \tag{4.5}$$

and (4.1a) as well as (4.4) give (4.3a).

Likewise, choosing $\boldsymbol{z}_h := (\mathbf{curl}\, \boldsymbol{y}_h^d - \mathbf{curl}\, \mu^{-1}\, \mathbf{curl}\, \boldsymbol{p}_h^* - \sigma \boldsymbol{p}_h^*) b_T$ in (2.2b), we find

$$\left(\eta_{p,T}^{(1)} \right)^2 \leq 2 h_T^2 \left(\left\| \mathbf{curl}\, \boldsymbol{y}_h^d - \mathbf{curl}\, \mu^{-1}\, \mathbf{curl}\, \boldsymbol{p}_h^* - \sigma \boldsymbol{p}_h^* \right\|_{0,T} + \| \mathbf{curl}(\boldsymbol{y}^d - \boldsymbol{y}_h^d) \|_{0,T} \right)$$

$$\lesssim 2 h_T^2 \left(\left(\mathbf{curl}(\boldsymbol{y}_h^d - \mathbf{curl}\, \boldsymbol{y}_h^*) - \mathbf{curl}\, \mu^{-1}\, \mathbf{curl}\, \boldsymbol{p}_h^* - \sigma \boldsymbol{p}_h^*, \boldsymbol{z}_h \right)_{0,T} + \| \mathbf{curl}(\boldsymbol{y}^d - \boldsymbol{y}_h^d) \|_{0,T} \right).$$

For the first term on the right-hand side we find

$$h_T^2 \left(\mathbf{curl}(\boldsymbol{y}_h^d - \mathbf{curl}\, \boldsymbol{y}_h^*) - \mathbf{curl}\, \mu^{-1}\, \mathbf{curl}\, \boldsymbol{p}_h^* - \sigma \boldsymbol{p}_h^*, \boldsymbol{z}_h \right)_{0,T}$$

$$= h_T^2 \left(\boldsymbol{y}_h^d - \mathbf{curl}\, \boldsymbol{y}_h^*, \mathbf{curl}\, \boldsymbol{z}_h \right)_{0,T} - a(\boldsymbol{p}_h^*, \boldsymbol{z}_h)$$

$$= h_T^2 \left(a(\boldsymbol{p}^* - \boldsymbol{p}_h^*, \boldsymbol{z}_h) + (\mathbf{curl}(\boldsymbol{y}_h^d - \boldsymbol{y}^d), \boldsymbol{z}_h)_{0,T} + (\mathbf{curl}(\boldsymbol{y}_h^* - \boldsymbol{y}^*), \mathbf{curl}\, \boldsymbol{z}_h)_{0,T} \right)$$

$$\lesssim h_T^2 \left(\| \boldsymbol{p}^* - \boldsymbol{p}_h^* \|_{curl,T} \| \boldsymbol{z}_h \|_{curl,T} + \| \mathbf{curl}(\boldsymbol{y}^d - \boldsymbol{y}_h^d) \|_{0,T} \| \boldsymbol{z}_h \|_{0,T} \right.$$

$$\left. + \| \mathbf{curl}(\boldsymbol{y}^* - \boldsymbol{y}_h^*) \|_{0,T} \| \mathbf{curl}\, \boldsymbol{z}_h \|_{0,T} \right).$$

Using again Young's inequality, (4.1a), and (4.5) allows to deduce (4.3b). □

Lemma 4.2 *Under the assumptions of Theorem 4.1, there holds*

$$\eta_{y,T}^{(2)} \lesssim \| \boldsymbol{y}^* - \boldsymbol{y}_h^* \|_{0,T} + \| \boldsymbol{u}^* - \boldsymbol{u}_h^* \|_{0,T} + osc_T(\boldsymbol{f}), \tag{4.6a}$$

$$\eta_{p,T}^{(2)} \lesssim \| \boldsymbol{p}^* - \boldsymbol{p}_h^* \|_{0,T}, \tag{4.6b}$$

for every $T \in \mathcal{T}_h(\Omega)$.

Proof From the definition of $\eta_{y,T}^{(2)}$ we see that

$$\left(\eta_{y,T}^{(2)} \right)^2 = h_T^2 \left\| \mathrm{div}(\boldsymbol{f} - \sigma \boldsymbol{y}_h^*) \right\|_{0,T}^2 \leq 2 \left(h_T^2 \left\| \mathrm{div}(\boldsymbol{f}_h - \sigma \boldsymbol{y}_h^*) \right\|_{0,T}^2 + osc_T^2(\boldsymbol{f}) \right).$$

For the estimation of the first term on the right-hand side we choose ∇z_h, where $z_h := \operatorname{div}(\sigma\, y_h^*)|_T b_T$, as an admissible test function in (2.2a). Taking advantage of $\operatorname{div}(u_h^*|_T) = 0$ and (4.1a), we find

$$
\begin{aligned}
\big\|\operatorname{div}(f_h - \sigma\, y_h^*)\big\|_{0,T}^2 &\lesssim h_T^2 \left(\operatorname{div}(f_h + u_h^* - \sigma\, y_h^*), z_h\right)_{0,T} \\
&= h_T^2(-f - u_h^* + \sigma\, y_h^*, \nabla z_h)_{0,T} + h_T^2(\operatorname{div}(f_h - f), z_h)_{0,T} \\
&= h_T^2\left((-f - u_h^* + (f + u^*), \nabla z_h)_{0,T} + (\sigma(y_h^* - y^*), \nabla z_h)_{0,T}\right) \\
&\quad + h_T^2(\operatorname{div}(f_h - f), z_h)_{0,T} \\
&\lesssim h_T^2\left(\|u - u_h^*\|_{0,T} + \|y^* - y_h^*\|_{0,T}\right)\|\nabla z_h\|_{0,T} + h_T^2\|\operatorname{div}(f_h - f)\|_{0,T}\|z_h\|_{0,T}.
\end{aligned}
$$

Then, we conclude by an application of Young's inequality, the inverse inequality

$$
\|\nabla z_h\|_{0,T} \lesssim h_T^{-1}\|z_h\|_{0,T},
$$

and (4.1a).

On the other hand ∇z_h, where $z_h := \operatorname{div}(\sigma\, p_h^*)|_T b_T$, is an admissible test function in (2.2b). Hence

$$
\begin{aligned}
\left(\eta_{p,T}^{(2)}\right)^2 &\lesssim h_T^2(\operatorname{div}(\sigma\, p_h^*), z_h)_{0,T} = h_T^2(\sigma\, p_h^*, \nabla z_h)_{0,T} \\
&= h_T^2\left(\sigma(p_h^* - p^*), \nabla z_h\right)_{0,T} \lesssim h_T^2\|p^* - p_h^*\|_{0,T}\|\nabla z_h\|_{0,T},
\end{aligned}
$$

and we deduce (4.6b) by the same arguments as before. $\qquad\square$

Lemma 4.3 *Under the assumptions of Theorem 4.1, there holds*

$$
\eta_{y,F}^{(1)} \lesssim \|y^* - y_h^*\|_{curl,T_+\cup T_-} + h_F \left\|u^* - u_h^*\right\|_{0,T_+\cup T_-} + \eta_{y,T_+}^{(1)} + \eta_{y,T_-}^{(1)}, \quad (4.7a)
$$
$$
\eta_{p,F}^{(1)} \lesssim \|p^* - p_h^*\|_{0,T_+\cup T_-} + \eta_{p,T_+}^{(1)} + \eta_{p,T_-}^{(1)}, \qquad (4.7b)
$$

for every $F \in \mathcal{F}_h(\Omega)$, $F = T_+ \cap T_-$, $T_\pm \in \mathcal{T}_h(\Omega)$.

Proof We extend $[\gamma_t(\mu^{-1}\mathbf{curl}\, y_h^*)]_F$ to a polynomial function $[\gamma_t(\mu^{-1}\,\mathbf{curl}\, y_h^*)]_{T_\pm}$ on $T_\pm$ such that

$$
\left\|[\gamma_t(\mu^{-1}\mathbf{curl}\, y_h^*)]_{T_\pm}\right\|_{0,T_\pm} \lesssim h_{T_\pm}\left\|[\gamma_t(\mu^{-1}\mathbf{curl}\, y_h^*)]_F\right\|_{0,F}. \qquad (4.8)
$$

Using (4.1b), Stokes' theorem, and the fact that the associated extension $\tilde{z}_h$ of $z_h := [\gamma_t(\mu^{-1}\mathbf{curl}\, y_h^*)]_F b_F$ is an admissible test function in (2.2a), we obtain

$$
\begin{aligned}
\left(\eta_{y,F}^{(1)}\right)^2 &\lesssim h_F\left([\gamma_t(\mu^{-1}\mathbf{curl}\, y_h^*)]_F, z_h\right)_{0,F} = h_F\left((-\mathbf{curl}\,\mu^{-1}\,\mathbf{curl}\, y_h^*, \tilde{z}_h)_{0,T_+\cup T_-}\right. \\
&+ \left.(\mu^{-1}\mathbf{curl}\, y_h^*, \mathbf{curl}\,\tilde{z}_h)_{0,T_+\cup T_-}\right) = h_F\left(f + u_h^* - \mathbf{curl}\,\mu^{-1}\,\mathbf{curl}\, y_h^* - \sigma\, y_h^*, \tilde{z}_h)_{0,T_+\cup T_-}\right.
\end{aligned}
$$

$$+ (\mu^{-1}\mathbf{curl}(y_h^* - y^*), \mathbf{curl}\,\tilde{z}_h)_{0,T_+\cup T_-} + (\sigma(y_h^* - y^*), \tilde{z}_h)_{0,T_+\cup T_-}$$

$$+ (u^* - u_h^*, \tilde{z}_h)_{0,T_+\cup T_-}\Big) \lesssim \Big(h_F\|\mathbf{curl}(y^* - y_h^*)\|_{0,T_+\cup T_-}\,\|\mathbf{curl}\,\tilde{z}_h\|_{0,T_+\cup T_-}$$

$$+ h_F\|y^* - y_h^*\|_{0,T_+\cup T_-}\,\|\tilde{z}_h\|_{0,T_+\cup T_-} + h_F\|u^* - u_h^*\|_{0,T_+\cup T_-}\,\|\tilde{z}_h\|_{0,T_+\cup T_-}$$

$$+ (\eta_{y,T_+} + \eta_{y,T_-})\|\tilde{z}_h\|_{0,T_+\cup T_-}\Big).$$

We deduce (4.7a) by Young's inequality, (4.1b), and (4.8). The proof of (4.7b) follows the same lines. □

Lemma 4.4 *Under the assumptions of Theorem 4.1, there holds*

$$\eta_{y,F}^{(2)} \lesssim \|y^* - y_h^*\|_{0,T_+\cup T_-} + \|u^* - u_h^*\|_{0,T_+\cup T_-} + \eta_{y,T_+}^{(2)} + \eta_{y,T_-}^{(2)} + osc_T(f),$$
(4.9a)

$$\eta_{p,F}^{(2)} \lesssim \|p^* - p_h^*\|_{0,T_+\cup T_-} + \eta_{p,T_+}^{(1)} + \eta_{p,T_-}^{(1)},$$
(4.9b)

for every $F \in \mathcal{F}_h(\Omega)$, $F = T_+ \cap T_-$, $T_\pm \in \mathcal{T}_h(\Omega)$.

Proof For every $F \in \mathcal{F}_h(\Omega)$, $F = T_+ \cap T_-$, $T_\pm \in \mathcal{T}_h(\Omega)$, we have

$$\left(\eta_{y,F}^{(2)}\right)^2 \leq 2h_F\left(\left\|n_F \cdot [f_h + u_h^* - \sigma y_h^*]_F\right\|_{0,F}^2 + \left\|n_F \cdot [f - f_h]_F\right\|_{0,F}^2\right). \quad (4.10)$$

As in the proof of (4.7a), we extend $n_F \cdot [f_h + u_h^* - \sigma y_h^*]_F$ to a polynomial function $n_F \cdot (f_h + u_h^* - \sigma y_h^*)_{T_\pm}$ on $T_\pm$ such that

$$\left\|n_F \cdot (f_h + u_h^* - \sigma y_h^*)_{T_\pm}\right\|_{0,T_\pm} \lesssim h_{T_\pm}\left\|n_F \cdot [f_h + u_h^* - \sigma y_h^*]_F\right\|_{0,F} \quad (4.11)$$

and take advantage of the fact that $\nabla\tilde{z}_h$, where $\tilde{z}_h$ stands for the associated extension of $z_h := n_F \cdot [f_h + u_h^* - \sigma y_h^*]_F b_F$, is an admissible test function in (2.2a). Using (4.1b), Green's formula and div $u_h^*|_{T_\pm} = 0$, it follows that

$$h_F\left\|n_F \cdot [f_h + u_h^* - \sigma y_h^*]_F\right\|_{0,F}^2 \lesssim h_F\left(n_F \cdot [f_h + u_h^* - \sigma y_h^*]_F, z_h\right)_{0,F}$$

$$= h_F\Big((\mathrm{div}(f_h + u_h^* - \sigma y_h^*), \tilde{z}_h)_{0,T_+\cup T_-} + (f_h + u_h^* - \sigma y_h^*, \nabla\tilde{z}_h)_{0,T_+\cup T_-}\Big)$$

$$= h_F\Big((\mathrm{div}(f - \sigma y_h^*), \tilde{z}_h)_{0,T_+\cup T_-} + (f_h + u_h^* - \sigma y_h^*, \nabla\tilde{z}_h)_{0,T_+\cup T_-}$$

$$+ (\mathrm{div}(f_h - f), \tilde{z}_h)_{0,T_+\cup T_-}\Big)$$

$$= h_F\Big((\mathrm{div}(f - \sigma y_h^*), \tilde{z}_h)_{0,T_+\cup T_-} + ((f_h - f) + (u_h^* - u^*)$$

$$-\sigma(y_h^* - y^*), \nabla\tilde{z}_h)_{0,T_+\cup T_-} + (\mathrm{div}(f_h - f), \tilde{z}_h)_{0,T_+\cup T_-}\Big)$$

$$\lesssim h_F\Big(\|y^* - y_h^*\|_{0,T_+\cup T_-}\,\|\nabla\tilde{z}_h\|_{0,T_+\cup T_-} + \|u^* - u_h^*\|_{0,T_+\cup T_-}\,\|\nabla\tilde{z}_h\|_{0,T_+\cup T_-}$$

$$+ (h_{T_+}^{-1} \eta_{y,T_+}^{(2)} + h_{T_-}^{-1} \eta_{y,T_-}^{(2)}) \|\tilde{z}_h\|_{0,T_+\cup T_-} + \|\boldsymbol{f} - \boldsymbol{f}_h\|_{0,T_+\cup T_-} \|\nabla\tilde{z}_h\|_{0,T_+\cup T_-}$$

$$+ \|\mathrm{div}(\boldsymbol{f} - \boldsymbol{f}_h)\|_{0,T_+\cup T_-} \|\tilde{z}_h\|_{0,T_+\cup T_-}\Big).$$

Young's inequality, (4.1b), and (4.10), (4.11) give rise to (4.9a). The proof of (4.9b) can be accomplished in a similar way. $\qquad\square$

5 Numerics

We consider two examples for the optimal control problem (2.1) with exact solutions featuring jump discontinuities and nonempty active sets. In the first example, we use a convex domain, whereas a nonconvex L-shaped domain is considered in the second one. All the numerical results presented below were implemented by a Python script using the Dolphin finite element library [27] and a projected gradient type method for solving the discrete optimality system. In the projected gradient type method, given a start iterate $\boldsymbol{u}_h^{(0)} \in \boldsymbol{K}_h$, in the n-th step ($n \geq 1$), we compute the solutions $\boldsymbol{y}_h^{(n)} \in \boldsymbol{V}_h$ and $\boldsymbol{p}_h^{(n)} \in \boldsymbol{V}_h$ of the discrete state Eq. (2.8a) and the discrete adjoint state Eq. (2.8b) with $\boldsymbol{u}_h^{(n-1)}$ in (2.9a) and $\boldsymbol{y}_h^{(n)}$ in (2.9b). We use the gradient Eq. (2.11) for the update

$$\hat{\boldsymbol{u}}_h^{(n-1)} := \boldsymbol{u}_h^{(n-1)} + \nu \, (\boldsymbol{p}_h^{(n)} - \alpha \left(\boldsymbol{u}_h^{(n-1)} - \boldsymbol{u}_h^d \right)),$$

where ν is the line search parameter. The projection onto the constraint set $\boldsymbol{K}_h$ proceeds as follows: Representing $\tilde{\boldsymbol{u}}_h^{n-1} \in \boldsymbol{V}_h$ according to

$$\hat{\boldsymbol{u}}_h^{n-1} = \sum_{j=1}^{N_h} U_j \, \boldsymbol{\varphi}_j,$$

where $\boldsymbol{\varphi}_j = (\varphi_{j,1}, \varphi_{j,2}, \varphi_{j,3})^T, 1 \leq j \leq N_h$, are the edge element basis functions associated with the edges of the triangulation, the constraint $\hat{\boldsymbol{u}}_h^{n-1} \geq \boldsymbol{0}$ is obviously satisfied, if for each nodal point $\boldsymbol{x}_k \in \mathcal{N}_h(\bar{\Omega}), 1 \leq k \leq M_h := \mathrm{card}(\mathcal{N}_h(\bar{\Omega}))$, and each tetrahedron $T_\ell \in \omega_{\boldsymbol{x}_k} := \bigcup \{T \in \mathcal{T}_h(\Omega) \mid \boldsymbol{x}_k \in \mathcal{N}_h(T)\}, 1 \leq \ell \leq L_k := \mathrm{card}(\omega_{\boldsymbol{x}_k})$, it holds

$$\sum_{j=1}^{N_h} U_j \, \varphi_{j,i}|_{T_\ell}(\boldsymbol{x}_k) \geq 0, \quad 1 \leq i \leq 3, \ 1 \leq k \leq M_h, \ 1 \leq \ell \leq L_k. \tag{5.1}$$

We set

$$b_{i,k,\ell} := \begin{cases} \sum_{j=1}^{N_h} U_j \, \varphi_{j,i}|_{T_\ell}(\boldsymbol{x}_k) & \text{if (5.1) is satisfied,} \\ 0 & \text{otherwise} \end{cases}$$

and determine $\bar{U} = (\bar{U}_1, \ldots, \bar{U}_{N_h})^T$ such that

$$\sum_{j=1}^{N_h} \bar{U}_j \, \varphi_{j,i}|_{T_\ell} (\boldsymbol{x}_k) = b_{i,k,\ell}, \quad 1 \le i \le 3, \ 1 \le k \le M_h, \ 1 \le \ell \le L_k. \quad (5.2)$$

We note that (5.2) represents an overdetermined linear algebraic system. In order to ensure feasibility, for the numerical solution we use an inequality constrained least-squares minimization. We finally set

$$\mathbf{u}_h^n = \sum_{j=1}^{N_h} \bar{U}_j \, \boldsymbol{\varphi}_j.$$

5.1 Convex domain

We consider a rather simple convex domain

$$\Omega = (-0.5, 0.5)^3.$$

However, the material parameters σ and μ^{-1} are chosen to be discontinuous as follows:

$$\sigma = \begin{cases} 100 & \text{in } \Omega_c, \\ 1 & \text{in } \Omega \setminus \Omega_c, \end{cases} \qquad \mu^{-1} = \begin{cases} 0.1 & \text{in } \Omega_c, \\ 1 & \text{in } \Omega \setminus \Omega_c, \end{cases}$$

with $\Omega_c := \{\boldsymbol{x} \in \mathbb{R}^3 \mid x_1^2 + x_2^2 + x_3^2 < 0.4^2\}$. Furthermore, the data involved in (2.1a)–(2.1b) are given by

$$\begin{cases} \alpha = 1, \\ \boldsymbol{y}^d \equiv \boldsymbol{\psi} \equiv (0, 0, 0)^T, \\ \boldsymbol{u}^d(\boldsymbol{x}) = 100(\chi_{\Omega_c}(\boldsymbol{x}), 0, 0)^T, \\ \boldsymbol{f}(\boldsymbol{x}) = \sigma \nabla \phi(\boldsymbol{x}) - 100(\chi_{\Omega_c}(\boldsymbol{x}), 0, 0)^T, \end{cases}$$

where χ_{Ω_c} denotes the characteristic function of Ω_c, and the scalar function ϕ is defined by

$$\phi(\boldsymbol{x}) := \frac{1}{2\pi} \sin(2\pi x_1) \sin(2\pi x_2) \sin(2\pi x_3).$$

Then, using the identity $\mathbf{curl} \, \nabla \equiv 0$, we infer that the unique solution for the optimal control problem (2.1) is given by

$$\boldsymbol{y}^* = \nabla \phi \quad \text{and} \quad \boldsymbol{u}^* = \boldsymbol{u}^d = 100(\chi_{\Omega_c}, 0, 0)^T.$$

We underline that the optimal control $\boldsymbol{u}^*$ features strong jump discontinuities across the interface $\partial \Omega_c$. Also, note that the lower bound $\boldsymbol{\psi}$ is *active* in $\Omega \setminus \Omega_c$ since

$$\boldsymbol{u}^*(\boldsymbol{x}) = \boldsymbol{\psi}(\boldsymbol{x}) \quad \text{in } \Omega \setminus \Omega_c.$$
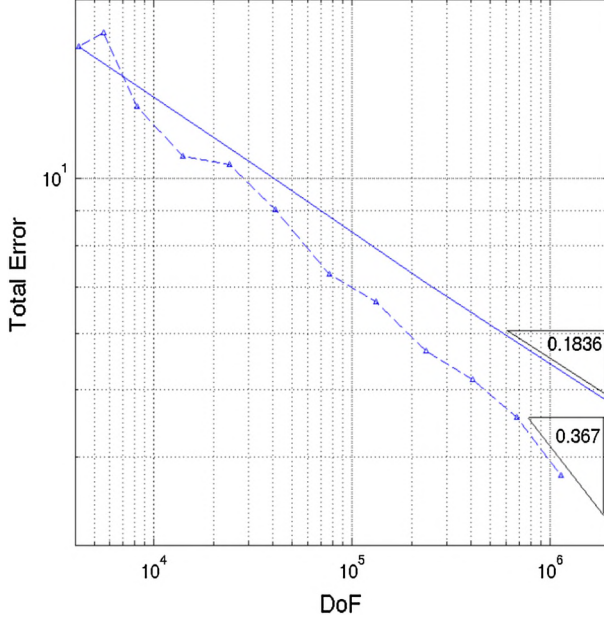
Fig. 1 Total error for uniform (*straight line*) and adaptive mesh refinement (*dash line*)
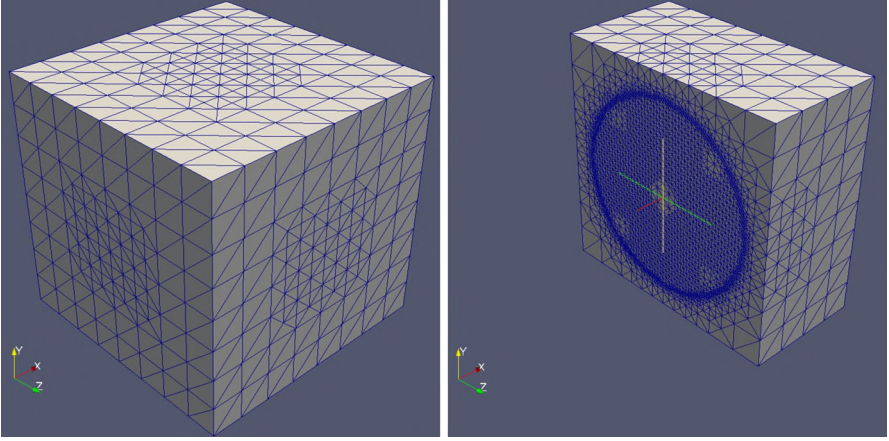

Fig. 2 Adaptive mesh

In Fig. 1, we report on the computed total error

$$\left\| \boldsymbol{y}^* - \boldsymbol{y}_h^* \right\|_{curl,\Omega} + \left\| \boldsymbol{p}^* - \boldsymbol{p}_h^* \right\|_{curl,\Omega} + \left\| \boldsymbol{u}^* - \boldsymbol{u}_h^* \right\|_{0,\Omega}$$

resulting from the uniform mesh refinement compared with the one based on the adaptive mesh refinement using the proposed error estimator η_h. Here, DoF denotes the degrees of freedom in the finite element space $\boldsymbol{V}_h$. The dependence of the total
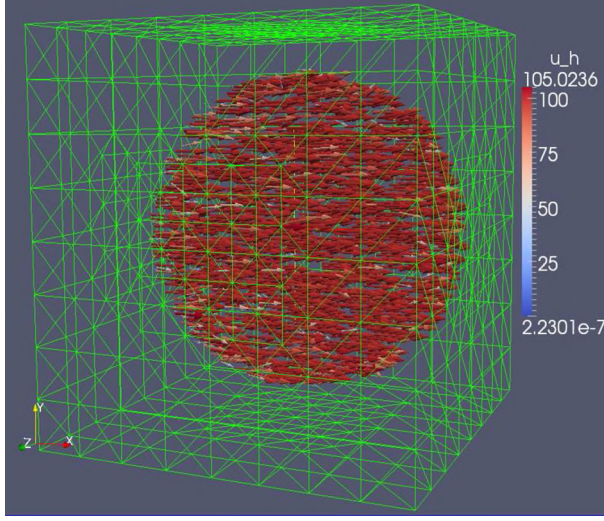
Fig. 3 Computed optimal control on the finest adaptive mesh

Table 1 Convergence history and effectivity index

DoF	$\|u^* - u_h^*\|_{0,\Omega}$	$\|y^* - y_h^*\|_{curl,\Omega}$	$\|p^* - p_h^*\|_{curl,\Omega}$	η_h	I_h
4,184	13.342150	0.5283963	1.5473114	76.495663	4.9614972
5,584	12.534318	0.6154268	2.9610072	71.288136	4.4248793
8,226	11.227854	0.3801630	1.0324547	55.668302	4.4039733
13,998	9.6861514	0.2776182	0.7903318	44.425982	4.1310733
24,022	8.8062130	0.2721502	1.3790808	41.991551	4.0154699
40,878	7.4791426	0.2517438	1.2801319	34.062026	3.7800418
76,734	6.7361067	0.1809946	0.3698392	27.037370	3.7103871
132,226	6.1216531	0.1699984	0.3596298	25.516922	3.8363919
236,356	5.0639413	0.1567532	0.4486637	20.833101	3.6746842
407,822	4.6930906	0.1473596	0.3256337	17.248254	3.3387483
680,408	4.2989472	0.1374215	0.1219806	16.021240	3.5147021
1140,498	3.5414586	0.1308141	0.0978973	13.099999	3.4746442

error on the DoF is shown on a double logarithmic scale. The number in the triangle marks the negative asymptotic slope of the curve. In case of adaptive refinement we asymptotically achieve optimal convergence. Note that the value $\theta = 0.8$ was used for the bulk criterion in the Dörfler marking. Furthermore, as plotted in Fig. 2, the adaptive mesh refinement is concentrated around the interface $\partial\Omega_c$. This behavior is expected as the optimal control u^* is constructed to have jump discontinuities across the interface $\partial\Omega_c$. Figure 3 displays the computed optimal control. Finally, Table 1 presents the convergence history of the adaptive method and the computed effectivity index
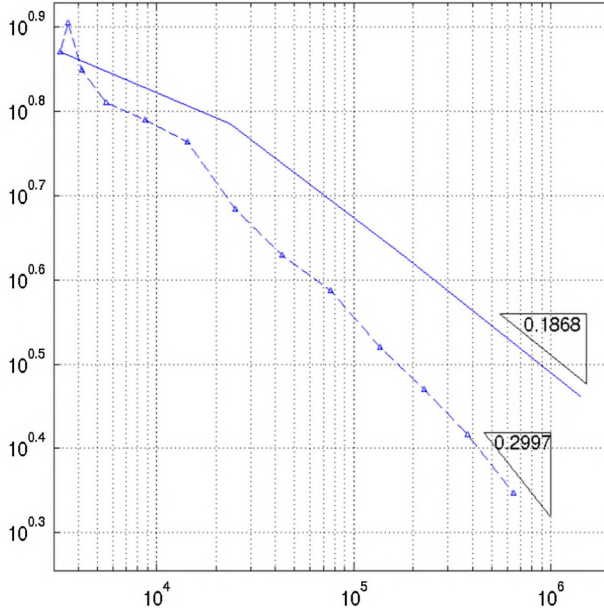
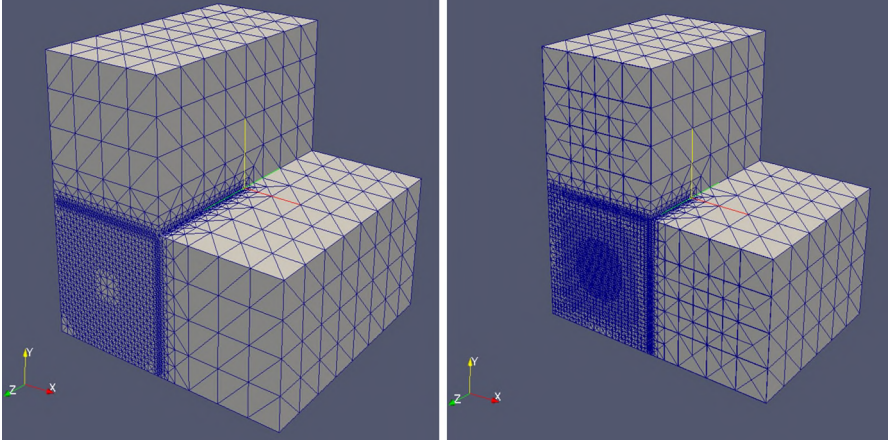**Fig. 4** Total error for uniform (*straight line*) and adaptive mesh refinement (*dash line*)
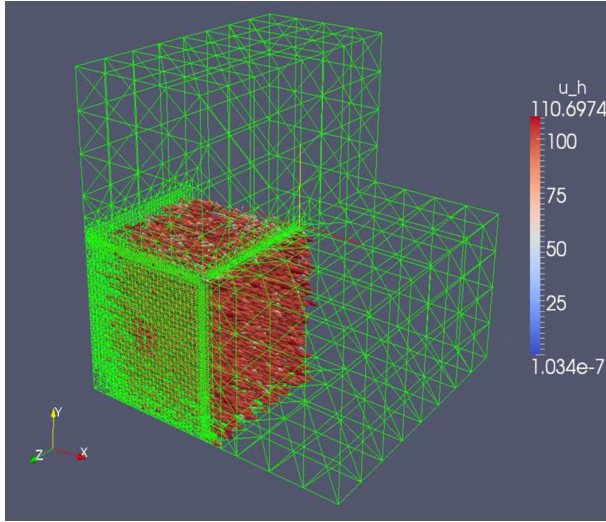

Fig. 5 Adaptive mesh

$$I_h = \frac{\eta_h}{\|\boldsymbol{y}^* - \boldsymbol{y}_h^*\|_{curl,\Omega} + \|\boldsymbol{p}^* - \boldsymbol{p}_h^*\|_{curl,\Omega} + \|\boldsymbol{u}^* - \boldsymbol{u}_h^*\|_{0,\Omega}}.$$

It is noticeable that the effectivity index I_h is around 3.7. We have also run this example with the regularization parameter $\alpha = 0.05$. As expected, the convergence of the projected gradient method slows down. However, there is only little impact on the effectivity index I_h which is around 3.5.

Table 2 Convergence history and effectivity index.

DoF	$\|\boldsymbol{u}^* - \boldsymbol{u}_h^*\|_{0,\Omega}$	$\|\boldsymbol{y}^* - \boldsymbol{y}_h^*\|_{curl,\Omega}$	$\|\boldsymbol{p}^* - \boldsymbol{p}_h^*\|_{curl,\Omega}$	η_h	I_h
3,240	6.2127131	0.3721735	0.8321832	47.340670	6.3826647
3,534	6.1671329	0.3908043	1.4826827	46.051480	5.7273543
4,180	5.8882736	0.3124360	0.8669483	37.542376	5.3118552
5,556	5.3860431	0.2838096	0.7875183	31.625600	4.8975967
8,723	4.9256000	0.2701240	0.9624568	28.329759	4.9256000
14,323	4.6266491	0.2500556	0.9228113	24.221931	4.1765434
25,121	3.9764198	0.2177334	0.6306379	19.530008	4.0478452
43,481	3.6083287	0.2036248	0.4464881	17.020006	3.9967685
76,517	3.2862561	0.1978778	0.3796225	14.924171	3.8626065
135,863	2.8060573	0.1875102	0.3223400	12.497666	3.7690030
228,820	2.5821776	0.1805546	0.1901377	10.743188	3.6382193
377,589	2.3214748	0.1597243	0.1268757	9.5684393	3.6687747
646,207	1.9855840	0.1284561	0.1061979	8.1414784	3.6669393

Fig. 6 Computed optimal control on the finest adaptive mesh

5.2 Nonconvex L-shaped domain

We consider now a nonconvex L-shaped computational domain

$$\Omega = (-0.5, 0.5)^3 \setminus \{(0, 0.5)^2 \times (-0.5, 0.5)\}.$$

Similarly to the first example, the material parameters σ and μ^{-1} are chosen to be discontinuous

$$\sigma = \begin{cases} 100 & \text{in } \Omega_c := (-0.5, 0)^2 \times (0, 0.5), \\ 1 & \text{otherwise,} \end{cases} \qquad \mu^{-1} = \begin{cases} 0.1 & \text{in } \Omega_c, \\ 1 & \text{otherwise.} \end{cases}$$

All other data are set as in the previous example. Due to the nonconvex structure of the computational domain, the convergence of the uniform mesh refinement method, compared with the previous example, becomes slower. This slow convergence is somewhat expected from the analysis, since solutions of curl–curl problems on nonconvex polyhedral domains feature singularities at reentrant corners (see [13]). Figure 4 again displays the dependence of the total error on the DoF on a double logarithmic scale. Due to the geometric singularity, for adaptive refinement we asymptotically expect optimal convergence rates around 0.3 which is confirmed by the numerical results. The adaptive method is also able to capture the region where jump discontinuities and singularities are present in the solution (see Fig. 5). The convergence history of the adaptive method is presented in Table 2. Here, the effectivity index is around 3.7. Finally, Fig. 6 displays the computed optimal control.

References

1. Ainsworth, M., Oden, T.: A Posteriori Error Estimation in Finite Element Analysis. Wiley, Chichester (2000)
2. Arnold, D., Falk, R., Winther, R.: Multigrid in H(div) and H(curl). Numer. Math. **85**, 197–217 (2000)
3. Arnold, D., Falk, R., Winther, R.: Finite element exterior calculus, homological techniques, and applications. Acta Numerica **15**(2006), 1–155 (2006)
4. Babuska, I., Strouboulis, T.: The Finite Element Method and its Reliability. Clarendon Press, Oxford (2001)
5. Bangerth, W., Rannacher, R.: Adaptive Finite Element Methods for Differential Equations. Lectures in Mathematics. ETH-Zürich. Birkhäuser, Basel (2003)
6. Beck, R., Deuflhard, P., Hiptmair, R., Hoppe, R.H.W., Wohlmuth, B.: Adaptive multilevel methods for edge element discretizations of Maxwell's equations. Surv. Math. Ind. **8**, 271–312 (1999)
7. Beck, R., Hiptmair, R., Hoppe, R.H.W., Wohlmuth, B.: Residual based a posteriori error estimators for eddy current computation. M2AN Math. Model. Numer. Anal. **34**, 159–182 (2000)
8. Binev, P., Dahmen, W., DeVore, R.: Adaptive finite element methods with convergence rates. Numer. Math. **97**, 219–268 (2004)
9. Buffa, A., Ciarlet Jr, P.: On traces for functional spaces related to Maxwell's equations. part i. Math. Meths. Appl. Sci. **24**, 9–30 (2001)
10. Carstensen, C., Hoppe, R.H.W.: Convergence analysis of an adaptive edge finite element method for the 2d eddy current equations. J. Numer. Math. **13**, 19–32 (2005)
11. Carstensen, C., Hoppe, R.H.W.: Unified framework for an a posteriori error analysis of non-standard finite element approximations of H(curl)-elliptic problems. J. Numer. Math. **17**, 27–44 (2009)
12. Cascon, J.M., Kreuzer, Ch., Nochetto, R.H., Siebert, K.G.: Quasi-optimal rate of convergence of adaptive finite element methods. SIAM J. Numer. Anal. **46**, 2524–2550 (2008)
13. Costabel, M., Dauge, M.: Singularities of electromagnetic fields in polyhedral domains. Arch. Ration. Mech. Anal. **151**, 221–276 (2000)
14. Dörfler, W.: A convergent adaptive algorithm for Poisson's equation. SIAM J. Numer. Anal. **33**, 1106–1124 (1996)
15. Eriksson, K., Estep, D., Hansbo, P., Johnson, C.: Computational Differential Equations. Cambridge University Press, Cambridge (1996)

16. Gaevskaya, A., Hoppe, R.H.W., Iliash, Y., Kieweg, M.: Convergence analysis of an adaptive finite element method for distributed control problems with control constraints. In: Leugering, G., et al., (eds.) Proc. Conf. Optimal Control for PDEs, Oberwolfach, Germany, Birkhäuser, Basel (2007)
17. Hintermüller, M., Hoppe, R.H.W.: Goal-oriented adaptivity in control constrained optimal control of partial differential equations. SIAM J. Control Optim. **47**, 1721–1743 (2008)
18. Hintermüller, M., Hoppe, R.H.W., Iliash, Y., Kieweg, M.: An a posteriori error analysis of adaptive finite element methods for distributed elliptic control problems with control constraints. ESAIM Control Optim. Calc. Var. **14**, 540–560 (2008)
19. Hiptmair, R.: Multigrid method for Maxwell's equations. SIAM J. Numer. Anal. **36**, 204–225 (1999)
20. Hiptmair, R.: Finite elements in computational electromagnetism. Acta Numerica **11**, 237–339 (2002)
21. Hiriart-Urruty, J.B., Lemaréchal, C.: Convex Analysis and Minimization Algorithms. Springer, Berlin-Heidelberg-New York (1993)
22. Hoppe, R.H.W., Schöberl, J.: Convergence of adaptive edge element methods for the 3d eddy currents equations. J. Comp. Math. **27**, 657–676 (2009)
23. Houston, P., Perugia, I., Schötzau, D.: A posteriori error estimation for discontinuous Galerkin discretizations of H(curl)-elliptic partial differential equations. IMA J. Numer. Anal. **27**, 122–150 (2007)
24. Kolmbauer, M., Langer, U.: A robust preconditioned minres solver for distributed time-periodic eddy current optimal control problems. SIAM J. Sci. Comput. **34**, B785–B809 (2012)
25. Li, R., Liu, W., Ma, H., Tang, T.: Adaptive finite element approximation for distributed elliptic optimal control problems. SIAM J. Control Optim. **41**, 1321–1349 (2002)
26. Liu, W., Yan, N.: Adaptive Finite Element Methods for Optimal Control Governed by PDEs. Series in Information and Computational Science, vol. 41. Global Science Press, Hong Kong (2008)
27. Logg, A., Mardal, K.-A., Wells, G.N.: Automated Solution of Differential Equations by the Finite Element Method. Springer, Boston (2012)
28. Monk, P.: A posteriori error indicators for Maxwell's equations. J. Comp. Appl. Math. **100**, 173–190 (1998)
29. Monk, P.: Finite Element Methods for Maxwell Equations. Oxford University Press, Oxford (2003)
30. Nédélec, J.-C.: Mixed finite elements in $\mathbb{R}^3$. Numer. Math. **35**, 315–341 (1980)
31. Neittaanmäki, P., Repin, S.: Reliable Methods for Mathematical Modelling. Error Control and a Posteriori Estimates. Elsevier, New York (2004)
32. Schöberl, J.: A posteriori error estimates for Maxwell equations. Math. Comp. **77**, 633–649 (2008)
33. Stevenson, R.: Optimality of a standard adaptive finite element method. Found. Comput. Math. **7**, 245–269 (2007)
34. Tartar, L.: Introduction to Sobolev Spaces and Interpolation Theory. Springer, Berlin (2007)
35. Tröltzsch, F.: Optimal Control of Partial Differential Equations. Theory, Methods, and Applications. American Mathematical Society, Providence (2010)
36. Tröltzsch, F., Yousept, I.: PDE-constrained optimization of time-dependent 3D electromagnetic induction heating by alternating voltages. ESAIM M2AN **46**, 709–729 (2012)
37. Verfürth, R.: A Review of a Posteriori Estimation and Adaptive Mesh—Refinement Techniques. Wiley-Teubner, New York (1996)
38. Vexler, B., Wollner, W.: Adaptive finite elements for elliptic optimization problems with control constraints. SIAM J. Control Optim. **47**, 1150–1177 (2008)
39. Zhong, L., Chen, L., Shu, S., Wittum, G., Xu, J.: Optimal error estimates of the Nedelec edge elements for time-harmonic Maxwell's equations. J. Comput. Math. **27**(2009), 563–572 (2009)
40. Yousept, I.: Optimal control of quasilinear **H(curl)**-elliptic partial differential equations in magnetostatic field problems. SIAM J. Control Optim. **51**, 3624–3651 (2013)
41. Yousept, I.: Optimal control of Maxwell's equations with regularized state constraints. Comput. Optim. Appl. **52**, 59–581 (2012)
42. Yousept, I.: Finite element analysis of an optimal control problem in the coefficients of time-harmonic eddy current equations. J. Optim. Theory Appl. **154**, 879–903 (2012)
43. Zhong, L., Chen, L., Shu, S., Wittum, G., Xu, J.: Convergence and optimality of adaptive edge finite element methods for time-harmonic Maxwell equations. Math. Comp. **81**, 623–642 (2012)